# Multiple breathers on a vortex filament



2014 J. Phys.: Conf. Ser. 544 012005

(http://iopscience.iop.org/1742-6596/544/1/012005)

Journal of Physics: Conference Series **544** (2014) 012005 doi:10.1088/1742-6596/544/1/012005

# Multiple breathers on a vortex filament

**H. Salman**[1]

[1] School of Mathematics, University of East Anglia, Norwich Research Park, Norwich, NR4 7TJ, UK

E-mail: H.Salman@uea.ac.uk

**Abstract.** In this paper we investigate the correspondence between the Da Rios-Betchov equation, which appears in the three-dimensional motion of a vortex filament, and the nonlinear Schrödinger equation. Using this correspondence we map a set of solutions corresponding to breathers in the nonlinear Schrödinger equation to waves propagating along a vortex filament. The work presented generalizes the recently derived family of vortex configurations associated with these breather solutions to a wider class of configurations that are associated with combination homoclinic/heteroclinic orbits of the 1D self-focussing nonlinear Schrödinger equation. We show that by considering these solutions of the governing nonlinear Schrödinger equation, highly nontrivial vortex filament configurations can be obtained that are associated with a pair of breather excitations. These configurations can lead to loop-like excitations emerging from an otherwise weakly perturbed helical vortex. The results presented further demonstrate the rich class of solutions that are supported by the Da Rios-Betchov equation that is recovered within the local induction approximation for the motion of a vortex filament.

## 1. Introduction

The vorticity representation of the equations of motion of a fluid is appealing in that it provides a direct understanding of the dynamics in terms of the rotational component of the velocity field associated with coherent vortex structures. In the limit of an ideal, inviscid fluid, fluid elements with non-zero vorticity evolve according to the Helmholtz laws of vortex motion which permits a geometric interpretation of the evolution of the vorticity field. This geometric interpretation is most succinctly illustrated in the case of a vortex filament which consists of vorticity of infinite strength concentrated along the length of the filament. In such a case, deformations or excitations created along the filament evolve in a non-trivial way due to the self-induced velocity produced by the instantaneous configuration of the filament. While the vortex filament concept is an attractive mathematical idealisation in the context of classical fluids, vortex filaments are physically real entities in superfluids. In this respect, understanding the fundamental type of excitations that can survive along these filaments becomes even more relevant as such excitations turn out to be the main degrees of freedom remaining in a superfluid in the ultra low temperature regime.

The study of excitations on a vortex dates back to the work of Kelvin (1880), who considered low amplitude perturbations of a straight vortex. These linear perturbations, now referred to as Kelvin waves, have been invoked by Vinen (2000); Kozik & Svistunov (2009); L'vov & Nazarenko (2010) to explain the dissipation mechanism in superfluids at extremely low temperatures. Kelvin waves can be recovered by truncating the full equations that govern the motion of a filament at leading order. In this approximation, the dynamics are governed by the local shape

of the filament and is, therefore, referred to as the local induction approximation (LIA). This approximation removes the nonlocal contributions arising from the Biot-Savart law by expressing the velocity field induced in terms of the local curvature. The governing equation of motion of a vortex then reduces to the Da Rios-Betchov equation (Rios, 1906; Betchov, 1965; Ricca, 1996). While Kelvin waves are the main low amplitude excitations, it is also important to consider larger amplitude excitations propagating along the filament. Such excitations can still be studied within the framework of the Da Rios-Betchov equation. The first analytical study in this direction was carried out by Hasimoto (1972) who showed that the LIA can be mapped onto the nonlinear Schrödinger equation (NLS) of the self-focusing type. This connection was profound since the NLS equation is known to be integrable and admits soliton solutions. The correspondence between the two implied that these solitons represent nonlinear excitations and have a corresponding geometric interpretation in the context of a vortex filament. Hasimoto presented an explicit expression for these soliton excitations propagating along a vortex and classified them into three different categories, a hump soliton, a cusp soliton, and a loop soliton depending on the relative magnitude of the curvature and torsion of the filament. The discovery of Hasimoto's solitons lead to a wealth of results on solitons on vortices (Konno *et al.*, 1991; Konno & Ichikawa, 1992; Leibovich & Ma, 1983). In particluar, we refer to the work of Hopfinger & Browand (1982), who observed these structures experimentally. This further illustrated that while the LIA neglects the full dynamics containd in the Biot-Savart law, the approximation can, nevertheless, be used to infer excitations that arise on real vortices. Subsequent work has lead to a number of generalisations of Hasimoto's work. This included a formulation by Cieśliński (1992) for two soliton solutions propagating along the filament as well as N-soliton solutions on a vortex (Fukumoto & Miyazaki, 1986; Levi *et al.*, 1983; Maksimović *et al.*, 2003).

Despite the progress made, there is much less work focused on the integrability of the Da Rios-Betchov equation of a vortex filament in comparison to the NLS equation. This is particularly true of integrable solutions of the NLS equation known as breathers. A breather is a nonlinear wave in which energy concentrates in a localized and oscillatory manner. Unlike solitons, breathers appear unsteady in any frame of reference. Breather solutions of the NLS equation were first predicted by Kuznetsov (1977) and Ma (1979) as a temporally periodic modulation, and by Akhmediev *et al.* (1987) as a spatially periodic modulation of a plane wave solution. A limiting case of these two solutions arises in the form of the Peregrine soliton (Peregrine, 1983) which is recovered either when the spacial period of the modulation of the Akhmediev breather tends to infinity or when the temporal period of the Ma-Kuznetsov breather tends to infinity (Dysthe & Trulsen, 1999). In contrast to solitons, which can arise both for the self-focusing and self-defocusing forms of the NLS equation and correspond to bright and dark solitons, respectively, breathers only occur in the former case. We note that the difference between the two equations arises from the relative signs of the nonlinear and dispersion terms. Since the Hasimoto transformation leads to an NLS equation of the self-focusing type, we would anticipate breather like excitations to arise in the case of the Da Rios-Betchov equations. It is, therefore, surprising that essentially no work has been carried out to investigate breathers in the case of vortex motion within the LIA. An exception to this is the work of Umeki (2010) who derived a set of equations permitting exact and explicit solutions to be obtained for the motion of the tangent vector of the vortex filament within the LIA. Umeki's work was motivated by the observation that the breather solutions obtained for the NLS equation are commonly presented in a form in which they are homoclinic to a spatially uniform plane wave. In the context of a vortex filament, this would imply that the excitations arise on an $n$-ply wound circular vortex which is somewhat unphysical. Umeki, therefore, worked directly with the Da Rios-Betchov equation obtaining an explicit solution for the tangent vector of the vortex filament. The vortex could then be reconstructed by direct numerical integration from this solution of the tangent vector. Very recently, Salman (2013) generalised the breather solutions by establishing a connection between

the breather solutions of the NLS equation and solutions of the Da Rios-Betchov equation. This approach has the advantage that it allows results already derived and established for the NLS equation to be mapped onto novel vortex configurations corresponding to these localised excitations. Using this mapping, Salman was able to illustrate how the Akhmediev breather solution maps onto loop like excitations of a periodic helical vortex. Moreover, he illustrated that these solutions persist even under the full dynamics of the Biot-Savart law where the loop-like excitations can ultimately induce a self-reconnection on the vortices. He also demonstrated these vortex excitations arise in a microscopic model of a superfluid provided by the mean field description of the Gross-Pitaevskii equation (Gross, 1961; Pitaevskii, 1961). The mechanism identified by Salman is distinct from other mechanisms previously discussed (e.g. Kursa *et al.* (2011)) for generating vortex loops. In particular, it is consistent with the aforementioned theories of the superfluid turbulence regimes identified.

Given the generality of the formulation presented in Salman (2013), we will extend the results to a more general class of breather solutions. In particular, we will consider how so-called combination homoclinic/heteroclinic solutions of the NLS, as derived by Ablowitz & Herbst (1990), map onto vortex configurations of the NLS equation. We point out that while Ablowitz & Herbst refer to these solutions as combination homoclinic orbits, Akhmediev & Korneev (1986) previously illustrated that the phase shifts that arise in such solutions are more appropriately described in terms of heteroclinic orbits. We will, therefore, refer to these solutions as homoclinic/heteroclinic orbits with the understanding that they are, in fact, associated with the same form of solution. Given that we have already established that in Salman (2013), the results of the LIA extend to more realistic models, we will focus exclusively on analysing our results for the Da Rios-Betchov equation.

## 2. The Da Rios-Betchov Equation and Hasimoto's Transformation

We begin by recalling that a vortex filament with circulation $\Gamma$ induces a velocity according to the Biot-Savart law given by

$$\mathbf{v}(\mathbf{r}) = \frac{\Gamma}{4\pi}\int_{\mathcal{C}(t)} \frac{d\mathbf{s}\times(\mathbf{r}-\mathbf{s})}{|\mathbf{r}-\mathbf{s}|^3}, \tag{1}$$

where $\mathbf{r}$ is the position vector for any point in the fluid, and the vector $\mathbf{s}$ runs along the vortex filament parameterised by the initial arclength $\xi$. The integral is evaluated along the curve $\mathcal{C}(t)$ that varies with time. This equation shows that the velocity induced on a superfluid vortex depends on the instantaneous configuration of a vortex line where non-local contributions arise from the terms under the integral. To simplify the problem, it can be shown Schwarz (1988); Donnelly (1991) that, at leading order, the vortex velocity depends on the local radius of curvature $R$ and the vortex core radius $a_o$ with

$$\dot{\mathbf{s}} = (\Gamma/4\pi)\ln(R/a_o)\mathbf{s}'\times\mathbf{s}'' \equiv \beta(\mathbf{s}'\times\mathbf{s}''), \tag{2}$$

where dot denotes partial differentiation with respect to time with $\xi$ held fixed, and primes denote partial differentiation with respect to arclength $\xi$ with time $t$ held fixed. Equation (2) corresponds to the Da Rios-Betchov equation of motion of a vortex filament. By introducing the Seret-Frenet equations given by (Pismen, 1999),

$$\mathbf{r}' = \mathbf{t}, \quad \mathbf{t}' = \kappa\mathbf{n}, \quad \mathbf{n}' = \tau\mathbf{b} - \kappa\mathbf{t}, \quad \mathbf{b}' = -\tau\mathbf{n}, \tag{3}$$

where $\mathbf{t}, \mathbf{n}, \mathbf{b}$ are a right-handed system of mutually perpendicular unit vectors corresponding to the tangent, the principal normal and binormal directions, respectively, Eq. (2) can be written as $\dot{\mathbf{r}} = \beta\kappa\mathbf{b}$. In general, although $\beta$ can vary since it depends on the radius of curvature $R$, it

will be assumed to be constant. Here, $\kappa(\xi,t)$ and $\tau(\xi,t)$ denote the local curvature and torsion of the filament, respectively. In order to transform Eq. (2) into a form corresponding to the NLS equation, we introduce the variables

$$\mathbf{N} = (\mathbf{n} + i\mathbf{b}) \exp\left( i \int_{\xi_p}^{\xi} \tau(\tilde{\xi}) d\tilde{\xi} \right), \quad \phi = \kappa \exp\left( i \int_{\xi_p}^{\xi} \tau(\tilde{\xi}) d\tilde{\xi} \right). \tag{4}$$

These two quantities are the intrinsic variables of the vortex and completely determine the configuration of the filament up to an arbitrary orientation in physical space.

Following the procedure set out in Hasimoto (1972), Eq. (2) can then be mapped to

$$\beta^{-1}(i\phi_t) = -\phi_{\xi\xi} - \frac{1}{2}|\phi|^2\phi. \tag{5}$$

We observe that the resulting equation is a self-focussing NLS equation and can, therefore, admit breather solutions. The breather solutions of this equation will be presented in the next section. In order to reconstruct the vortex from the function $\phi(\xi,t)$, the orientation and position of the vortex is specified at a particular instant in time. A procedure is then required whereby the location and orientation of the vortex must be recovered from the equation of motion self-consistently. To accomplish this, we revert back to the Seret-Frenet equations (3) and consider the time derivatives of the tangent vector $\mathbf{t}$ and the complex vector $\mathbf{N}$ to obtain

$$\dot{\mathbf{t}} = \frac{1}{2}\left(\phi'\overline{\mathbf{N}} - \overline{\phi'}\mathbf{N}\right), \quad \dot{\mathbf{N}} = \frac{i}{2}\left(\kappa^2\mathbf{N} - 2\phi'\mathbf{t}\right). \tag{6}$$

Here, bars denote complex conjugate quantities. To simplify the prescription of the initial tangent, normal, and binormal vectors, we will choose a point on the vortex filament that coincides with the point $\xi = \xi_p(t)$ such that $\kappa'(\xi_p) = 0$. Therefore, given the initial condition at time $t_i$ for the vectors $\mathbf{t}(\xi_p(t_i))$, $\mathbf{n}(\xi_p(t_i))$, $\mathbf{b}(\xi_p(t_i))$, we must evaluate these vectors at some later time $t$. This would provide the initial conditions to determine the constant of integration of the Seret-Frenet system of equations. To obtain the desired equations for the change of $\mathbf{t}$ and $\mathbf{N}$ moving along the point $\xi_p(t)$, we simply consider the rate of change $\frac{D}{Dt} = \frac{\partial}{\partial t}\big|_s + 2\tau_o \frac{\partial}{\partial s}\big|_t$ where $\tau_o$ is a constant torsion associated with the unperturbed helical vortex filament as derived in the following section. The equations describing the rate of change of the three vectors of the Seret-Frenet system can then be cast in the form

$$\frac{D}{Dt}\begin{pmatrix} \sqrt{2}\mathbf{t} \\ \mathbf{N} \\ \overline{\mathbf{N}} \end{pmatrix} = \begin{pmatrix} \mathbf{0} & -\overline{h}\mathbf{I} & -h\mathbf{I} \\ h\mathbf{I} & \frac{i\kappa^2}{2}\mathbf{I} & \mathbf{0} \\ \overline{h}\mathbf{I} & \mathbf{0} & -\frac{i\kappa^2}{2}\mathbf{I} \end{pmatrix} \begin{pmatrix} \sqrt{2}\mathbf{t} \\ \mathbf{N} \\ \overline{\mathbf{N}} \end{pmatrix}, \tag{7}$$

where, $h(s) = -\left(i\phi'/\sqrt{2} + \sqrt{2}\tau_o\phi\right)$, and $\mathbf{0}$ and $\mathbf{I}$ are $3\times3$ zero and identity matrices, respectively. We have written the governing equations in skew-Hermitian form which arises as a consequence of the underlying symplectic structure of the LIA. The algorithm prescribed above permits complete reconstruction of the vortex. We will now consider the class of breather solutions that are associated with the function $\phi$.

## 3. Breathers of the Nonlinear Schrödinger Equation

The main breather solutions covered in the literature come in two different types; the Kuznetsov-Ma breather (Kuznetsov, 1977; Ma, 1979) which has a temporally periodic solution, and the Akhmediev breather which is spatially periodic. In this work, we will be primarily interested in vortices that have a periodic structure along their arclength. For this reason, we will focus on

the Akhmediev breather solution, which will turn out to be more relevant for our considerations. The Akhmediev breather solution is typically cast in a form that corresponds to an orbit that is homoclinic/heteroclinic to a spatially uniform plane wave fixed point and is given by (Dysthe & Trulsen, 1999)

$$\begin{aligned}\phi_A(\xi,t) &= \mathrm{e}^{i\beta t/2}\frac{\cosh(\Omega\beta t/4-2i\varphi)-\cos(\varphi)\cos(k\xi/2)}{\cosh(\Omega\beta t/4)-\cos(\varphi)\cos(k\xi/2)},\\ k &= 2\sin(\varphi), \qquad \Omega = 2\sin(2\varphi).\end{aligned} \tag{8}$$

When interpreting this form of the solution in terms of a vortex, the basic state of the solution has no torsion and so would not correspond to vortices that are of general interest in classical fluids or superfluids. In order to generalise the above solution to a helical vortex, what is needed is an expression for a homoclinic/heteroclinic orbit to a spatially travelling plane wave solution. We can obtain such a solution by making use of two transformations satisfied by the NLS equation. Specifically, we note that Eq. (5) is invariant under the Galilean (gauge) and scaling transformations given respectively by

$$\begin{aligned}&t\to t, \quad \xi\to\xi-2\tau_o t, \quad \phi\to\phi\exp[i(\tau_o\xi-\tau_o^2 t)],\\ &t\to\kappa_o^2 t, \quad \xi\to\kappa_o\xi, \quad \phi\to\kappa_o\phi(\kappa_o\xi,\kappa_o^2 t).\end{aligned} \tag{9}$$

We note that under the above Galilean transformation, the spatially uniform plane wave solution maps onto a solution that corresponds to an unperturbed helical vortex with curvature $\kappa_o$ and torsion $\tau_o$. The breather solution we seek can, therefore, be recovered from Eq. (8) following these transformations to obtain

$$\phi_A(\xi,t)=\kappa_o\mathrm{e}^{i\kappa_o^2\beta t/2+i\tau_o\xi+i(\kappa_o^2-\tau_o^2)\beta t}\frac{\cosh(\Omega\kappa_o^2\beta t/4-2i\varphi)-\cos(\varphi)\cos(k\kappa_o\xi/2-k\tau_o\kappa_o\beta t)}{\cosh(\Omega\kappa_o^2\beta t/4)-\cos(\varphi)\cos(k\kappa_o\xi/2-k\tau_o\kappa_o\beta t)}. \tag{10}$$

This breather solution was considereded in Salman (2013) to study nonlinear excitations in the Da Rios-Betchov equation, the Biot-Savart law, and the Gross-Pitaevskii model of a superfluid. We note that a particulalry important solution of the Akhmediev breather arises in the limit $k\to 0$. In this case, we obtain the analogue of the Peregrine soliton given by

$$\phi_p=\lim_{k\to 0}q_A \;=\; \kappa_o\mathrm{e}^{i\tau_o\xi+i(\kappa_o^2-\tau_o^2)\beta t}\left\{1-\frac{4(1+i\kappa_o^2\beta t)}{1+4(\kappa_o\xi/2-\tau_o\kappa_o\beta t)^2+i(\kappa_o^2\beta t)^2}\right\}. \tag{11}$$

This solution has the maximum possible amplitude of $\phi$ (equivalently maximum curvature for the vortex) among the family of breather solutions given by Eq. (10).

The above Akhmediev breather solution was subsequently derived by Ablowitz and Herbst using the direct bilinear method of Hirota (1978, 1982). They expressed the solution in the form $\phi(\xi,t)=G(\xi,t)/F(\xi,t)$. By invoking the transformation given in Eq. (9), the expressions for G and F given in Ablowitz & Herbst (1990) transform to

$$\begin{aligned}G(\xi,t) &= \kappa_o\exp(i\kappa_o^2\beta t/2+i\tau_o\xi+i(\kappa_o^2-\tau_o^2)\beta t)\times\\ &\quad\left\{1+2\cos(\eta)\exp(\Omega\kappa_o^2\beta t/4+2i\phi+\gamma)+\frac{\exp(\Omega\kappa_o^2\beta t/2+4i\phi+2\gamma)}{(\cos^2\phi)}\right\},\\ F(\xi,t) &= \left\{1+2\cos(\eta)\exp(\Omega\kappa_o^2\beta t/4+\gamma)+\frac{\exp(\Omega\kappa_o^2\beta t/2+2\gamma)}{(\cos^2\phi)}\right\},\end{aligned} \tag{12}$$

where $\eta=k\kappa_o\xi/2-k\tau_o\kappa_o\beta t$, $\Omega=\pm k\sqrt{4-k^2}$ and $\gamma$ is an arbitrary phase. We note that by setting $\gamma=\log(-\cos(\phi))$ and choosing the negative root of $\Omega$, we recover the expression given

in Eq. (10). We, therefore, see that the form given in Eq. (12) is equivalent to the breather solution discussed above.

Using this form of solution, we can now also consider a pair of breather solutions also referred to in Ablowitz & Herbst (1990) as combination homoclinic orbits. In this case, the solution is given by

$$
\begin{aligned}
\phi(\xi,t) &= \kappa_o \mathrm{e}^{(i\kappa_o^2\beta t/2 + i\tau_o\xi + i(\kappa_o^2-\tau_o^2)\beta t)}\frac{G(\xi,t)}{F(\xi,t)} \\
G(\xi,t) &= 1 + 2\exp(-2i\phi_1)\cos(\eta_1)\exp(\Omega_1\kappa_o^2\beta t/4+\gamma_1) + A_{12}\exp(4i\phi_1)\exp(\Omega_1\kappa_o^2\beta t/2+2\gamma_1) \\
&\quad +2\exp(-2i\phi_3)\cos(\eta_3)\exp(\Omega_3\kappa_o^2\beta t/4+\gamma_3) + A_{34}\exp(4i\phi_3)\exp(\Omega_3\kappa_o^2\beta t/2+2\gamma_3) \\
&\quad +2\exp[-2i(\phi_1+\phi_3)]\,[A_{13}\cos(\eta_1+\eta_3) + A_{23}\cos(\eta_1-\eta_3)] \\
&\qquad \times \exp[(\Omega_1+\Omega_3)\kappa_o^2\beta t/4 + (\gamma_1+\gamma_3)] \\
&\quad +2A_{13}A_{23}A_{34}\exp[-i(2\phi_1+4\phi_3)]\cos(\eta_1)\exp[(\Omega_1+2\Omega_3)\kappa_o^2\beta t/4+(\gamma_1+2\gamma_3)] \\
&\quad +2A_{12}A_{13}A_{23}\exp[-i(4\phi_1+2\phi_3)]\cos(\eta_3)\exp[(2\Omega_1+\Omega_3)\kappa_o^2\beta t/4+(2\gamma_1+\gamma_3)] \\
&\quad +A_{12}A_{13}^2A_{23}^2A_{34}\exp[-4i(\phi_1+\phi_3)]\exp[2(\Omega_1+\Omega_3)\kappa_o^2\beta t/4+2(\gamma_1+\gamma_3)] \\
\\
F(\xi,t) &= 1 + 2\cos(\eta_1)\exp(\Omega_1\kappa_o^2\beta t/4+\gamma_1) + A_{12}\exp(4i\phi_1)\exp(\Omega_1\kappa_o^2\beta t/2+2\gamma_1) \\
&\quad +2\cos(\eta_3)\exp(\Omega_3\kappa_o^2\beta t/4+\gamma_3) + A_{34}\exp(4i\phi_3)\exp(\Omega_3\kappa_o^2\beta t/2+2\gamma_3) \\
&\quad +2\,[A_{13}\cos(\eta_1+\eta_3) + A_{23}\cos(\eta_1-\eta_3)] \\
&\qquad \times \exp[(\Omega_1+\Omega_3)\kappa_o^2\beta t/4 + (\gamma_1+\gamma_3)] \\
&\quad +2A_{13}A_{23}A_{34}\cos(\eta_1)\exp[(\Omega_1+2\Omega_3)\kappa_o^2\beta t/4+(\gamma_1+2\gamma_3)] \\
&\quad +2A_{12}A_{13}A_{23}\cos(\eta_3)\exp[(2\Omega_1+\Omega_3)\kappa_o^2\beta t/4+(2\gamma_1+\gamma_3)] \\
&\quad +A_{12}A_{13}^2A_{23}^2A_{34}\exp[2(\Omega_1+\Omega_3)\kappa_o^2\beta t/4+2(\gamma_1+\gamma_3)] \qquad (13)
\end{aligned}
$$

where

$$
\begin{aligned}
&A_{jk} = \left(\frac{\sin\frac{1}{2}(\Phi_j-\Phi_k)}{\sin\frac{1}{2}(\Phi_j+\Phi_k)}\right)^2, \quad \eta_i = k_i\kappa_o\xi/2 - k_i\tau_o\kappa_o\beta t, \quad k_i = 2\sin\Phi_i, \\
&\Omega_i = k_i\sqrt{4-k_i^2}, \quad \Phi_2 = \Phi_1+\pi, \quad \Phi_4 = \Phi_3+\pi. \qquad (14)
\end{aligned}
$$

In the next section we will present examples of breather excitations on vortices constructed from the above breather solutions. However, we point out that a general expression for constructing an even more complex set of breather solutions was presented in Ablowitz & Herbst (1990). Therefore, in principle, the method presented here could be applied to these breathers also.

## 4. Results

We begin by illustrating the breather solution given by Eq. (10). We have set $\kappa_o = r/(r^2+h^2)$, and $\tau_o = h/(r^2+h^2)$ where $r = 10$, $h = L/(2\pi n_H)$, $n_H = 6$ and $L = 128$, and set $\beta = 4\pi$. Figure (1a) shows how the curvature along the filament varies with time. Initially, the curvature is constant along the filament and corresponds to a helical vortex. As $t \to 0$, we observe the emergence of large deviations from the ambient level. The curvature eventually relaxes back to the background value as $t \to \infty$. Now looking at the plot of the torsion, presented in Fig. (1b), we notice that torsion is essentially a nonzero constant at early times. However, peaked values of the torsion (both positive and negative) emerge as $t \to 0$ which eventually relax back to $\tau_o$ for large times. We note that the values of these peaks are dependent on the resolution of the grid used to generate these surface plots of $\tau$ as a function of $(\xi, t)$ which in this case was set to

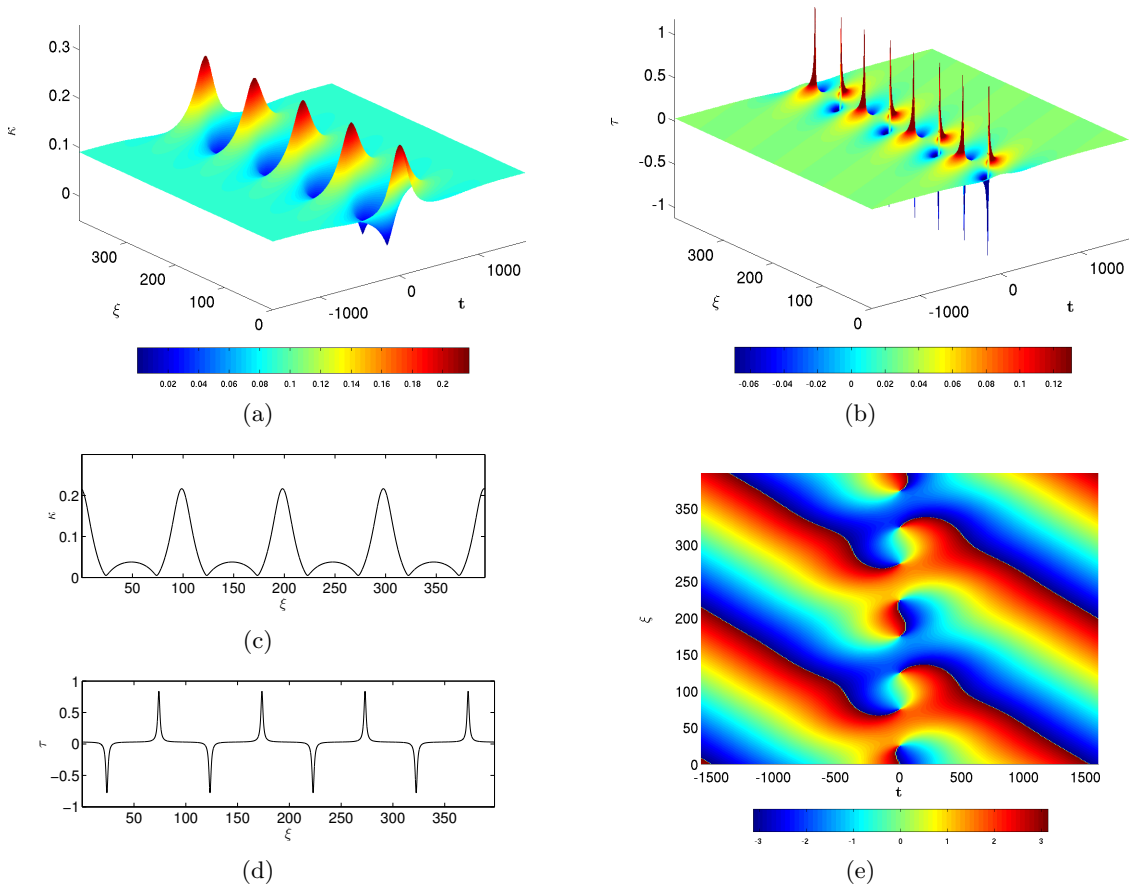


**Figure 1.** Akhmediev breather solution of the NLS equation for a travelling plane wave solution; (a) Temporal evoluation of amplitude of wavefunction, $\kappa$; (b) Temporal evoluation of gradient of phase of wavefunction, $\tau$; (c) Variation of $\kappa(\xi)$ at $t = 0$; (d) Variation of $\tau(\xi)$ at $t = -0.1\beta$; (e) Temporal evolution of phase of wavefunction.

$(\Delta\xi, \Delta t) = (0.01, 10)$. This indicates that a singular behaviour in the value of $\tau$ is reached as $t \to 0$ is approached. To understand this behaviour more fully, we have presented plots in Figs. (1c,d) of $\kappa$ and $\tau$ as a function of $\xi$ at $t = 0$ and $t = -0.1\beta$, respectively.

We note that at $t = 0$, the curvature vanishes at eight points along the length of the filament. Comparing with the plot of $\tau$, we observe that these correspond to peaked structures which, in fact, approach delta functions as $t \to 0$. The singular behaviour of $\tau$ is more evident in the phase plot of $\phi_A$ presented in Fig. (1e) as a function of arclength $\xi$ and time $t$. The figure clearly illustrates that the phase becomes ill defined at the points where $\kappa = 0$. Therefore, constructing the filament at $t = 0$ becomes problematic. To uncover the physical implication of this singular behaviour in the solution, we will now present the configuration of the vortex filament associated with these functions of $\kappa(\xi, t)$ and $\tau(\xi, t)$. Given our choice of parameters, we expect that in the limit $t \to \pm\infty$, we will have a helical vortex which can be parameterised as

$$x = x_o + r\cos\left(\frac{2\pi n_H \xi}{AL}\right), \quad y = y_o + r\sin\left(\frac{2\pi n_H \xi}{AL}\right), \quad z = \frac{\xi}{A},$$

where $A = \left[1 + (2\pi n_H/L)^2 r^2\right]^{1/2}$. The helical vortex contains 6 waves extending along the $z$-direction over an interval of length $L$ and with an amplitude, $r$. The vortex can be clearly seen in Fig. (2) which deforms as the breather solution is approached as $t \to 0$. As can be

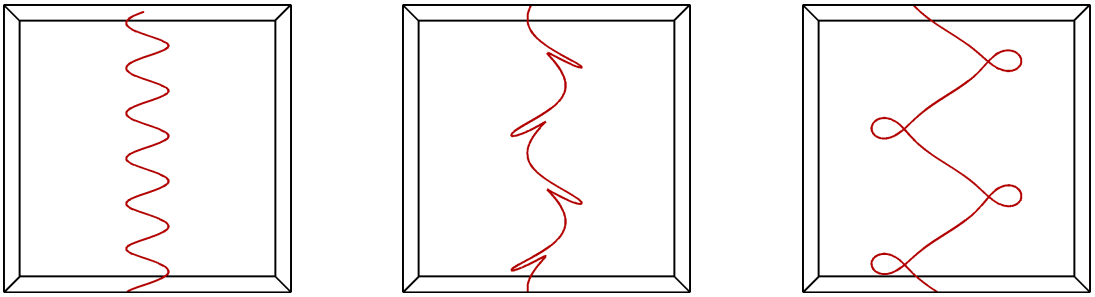

(a) $t = -800\beta$ (b) $t = -20\beta$ (c) $t = -0.1\beta$

**Figure 2.** Configuration of vortex filament corresponding to the Akhmediev breather at different times. Horizontal and vertical directions correspond to $x$ and $z$ coordinates respectively and depth corresponds to the $y$ coordinate.

seen, the breather is spatially periodic with a wavenumber of the spacial modulation given by $k = 4\pi n_B/(L\kappa_o)$ with $n_B = 4$. Near $t = 0$, we see loop like excitations. Upon more careful inspection, it becomes clear that the points corresponding to $\kappa = 0$ correspond to the severe twisting that the vortex experiences near $t = 0$. This provides the physical interpretation for the lack of a well defined torsion in this case. The breather solutions we have obtained for the vortex, therefore, provide a mechanism for generating vortex loops from a vortex. Indeed, this was confirmed in Salman (2013) with numerical simulations based on the Biot-Savart law and the Gross-Pitaevskii equation.

We pointed out in Section (3) that a particularly important limit of a breather is recovered in the limit $k \to 0$ and corresponds to the so-called Peregrine soliton given by Eq. (11). In the context of rogue waves in the ocean, the Peregrine soliton corresponds to a wave of maximum amplitude that can arise from the family of these breather solutions. In the context of vortices, this would imply breather excitations with maximum curvature emerging from the weakly perturbed helical vortex. We illustrate this case in Fig. (3a) where we clearly see a localised excitation in the function $\kappa(\xi, t)$ emerging as $t \to 0$. The corresponding plots for $\kappa$ at $t = 0$ and $\tau$ at $t = -0.1\beta$ are also included in Figs. (3b,c), respectively. We note that the maximum value of $\kappa$ at $t = 0$, is larger than the corresponding value presented for the breather in Fig. (3c) as expected for the Peregrine soliton Dysthe & Trulsen (1999). The corresponding vortex configuration presented in Fig. (4) now admits a single loop-like excitation since we are dealing with the limiting case where the wavenumber of the breathing mode tends to zero and so the spatial periodicity of the solution is lost.

We will now consider the multiple breather solutions presented in Eqs. (12) and (13). This case contains a larger number of parameters as the breathers can have different modulation wavenumbers, and can be offset with respect to one another in time. We will consider a particular example corresponding to $\gamma_1 = \gamma_2 = 0$ which displays quite complex spatio-temporal behaviour in the breathing modes. All other parameters are the same as the Akhmediev breather. In Fig. (5c), we present a surface plot of the curvature as a function of arclength and time. The solution now clearly exhibits much more complex behaviour than the Akhmediev breather solution. In particular, we note that the peaks that form emerge at different times and in different locations. This is also clearly reflected in the phase plot presented in Fig. (5d) that reveals the points where the curvature vanishes and where multiple self-reconnection events would be expected. To illustrate the non-trivial property of the vortex configurations associated with such breather solutions, we have plotted in Fig. (6) the vortex filament configurations corresponding to these breathers. Given our parameters, we point out that the initial vortex configuration at early times is the same as that presented in Fig. (2a). However, significant differences emerge at later

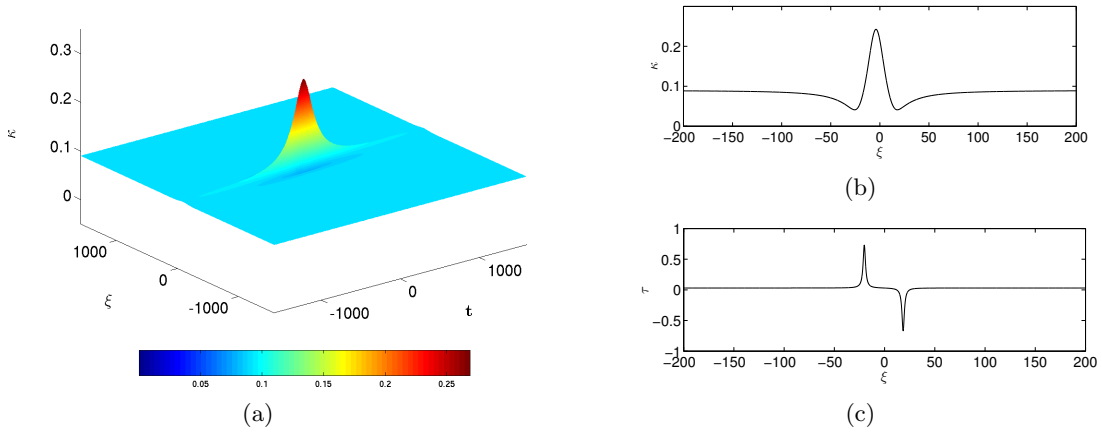


**Figure 3.** Peregrine solution of the NLS equation for a travelling plane wave solution; (a) Temporal evoluation of amplitude of wavefunction, $\kappa$; (b) Variation of $\kappa(\xi)$ at $t = 0$; (c) Variation of $\tau(\xi)$ at $t = -0.1\beta$.

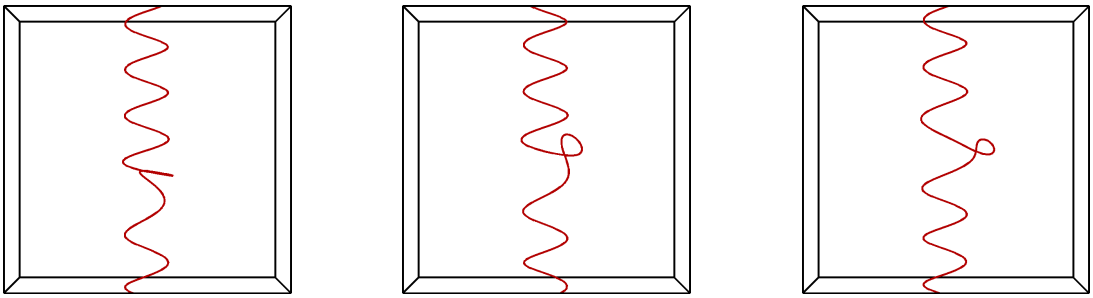

(a) $t = -20\beta$ (b) $t = -10\beta$ (c) $t = -0.1\beta$

**Figure 4.** Configuration of vortex filament corresponding to Peregrine soliton at different times. Horizontal and vertical directions correspond to $x$ and $z$ coordinates respectively and depth corresponds to the $y$ coordinate.

times in that the vortex loops that emerge lack the more regular structures observed with the Akhmediev breather. Moreover, different sized loop-like excitations emerge at different times indicating a more irregular and complex evolution of the vortex with time. While reconnections, do not arise in our simple LIA description presented here, based on our previous work, we would expect the dynamics observed from this simple model to generalize to models based on the Biot-Savart law or the Gross-Pitaevskii equation.

## 5. Conclusions

We have considered breather solutions of the Da Rios-Betchov equation which governs the motion of a vortex filament in the localised induction approximation. Using the correspondence between this equation and the self-focusing NLS equation that emerges upon application of Hasimoto's transformation, we have presented a method for mapping breather solutions of the NLS equation to the vortex filament. This approach has the benefit that it permits direct application of previously derived breather solutions of the nonlinear Schrödinger (NLS) equation to reconstruct the corresponding vortex configurations. To demonstrate our approach, we have considered three particular solutions of the NLS equation. This included the Akhmediev breather for a spatially traveling plane wave, the Peregrine soliton that is recovered when the period of the spacial modulation tends to infinity, and finally a pair of breather solutions that is recovered from

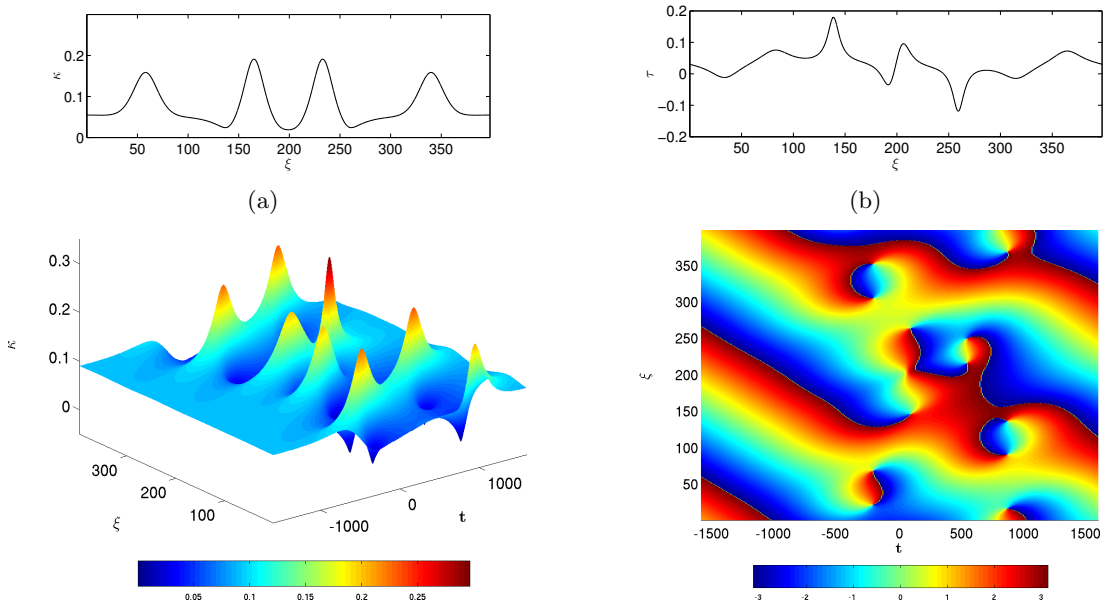


**Figure 5.** Multiple breather solution of the NLS equation for a travelling plane wave solution; (a) Temporal evoluation of amplitude of wavefunction, $\kappa$; (b) Temporal evoluation of gradient of phase of wavefunction, $\tau$; (c) Variation of $\kappa(\xi)$ at $t = 0$; (d) Variation of $\tau(\xi)$ at $t = -0.1\beta$; (e) Temporal evolution of phase of wavefunction.

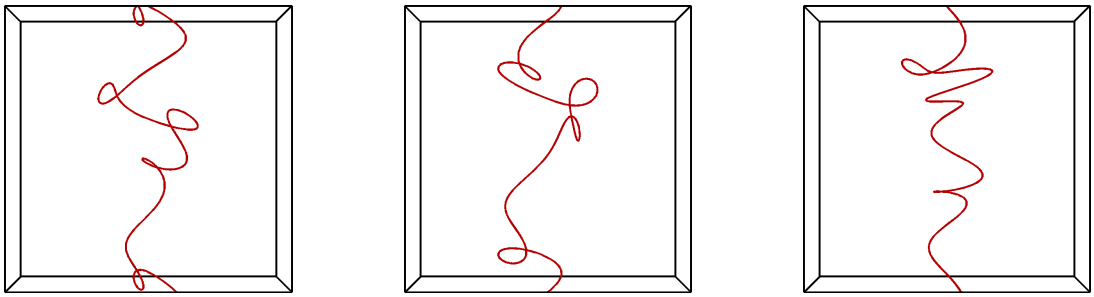

(a) $t = -15\beta$ (b) $t = 0$ (c) $t = 40\beta$

**Figure 6.** Configuration of vortex filament corresponding to a multiple breather at different times. Horizontal and vertical directions correspond to $x$ and $z$ coordinates respectively and depth corresponds to the $y$ coordinate.

a more general class of solutions permitting the construction of multiple breather excitations on a vortex filament. Our results clearly demonstrated that such excitations propagate along the filament giving rise to loop-like structures. Since our analysis was based exclusively on the localised induction approximation, no self-reconnections and change of topology arises in this model. However, the recent work presented in Salman (2013) clearly illustrates that when these excitations are considered in more realistic models of a vortex, such as the Biot-Savart law, the emergent loops lead to self-recrossings and the subsequent emission of vortex rings. This change in topology of the vortex that occurs in the nonlinear stages of the instability identified here can play an impotant role in how vortices release the excess energy stored within them. Such considerations can have important implications in a number of different physical contexts with the energy cascade in superfluid turbulence of liquid $^4$He being among one of the main potential

applications of the new theoretical results presented here.

## References

Ablowitz, M.J. & Herbst, B.M. 1990 On homoclinic structure and numerically induced chaos for the nonlinear schrödinger equation. *SIAM Journal of Applied Mathematics* **50**, 339.

Akhmediev, N.N., Eleonskii, V.M. & Kulagin, N.E. 1987 Exact first-order solutions of the nonlinear schrödinger equation. *Translation from Teoreticheskaya i Matematicheskaya Fizika* **72**, 183.

Akhmediev, N.N. & Korneev, V.I. 1986 Modulation instability and periodic solutions of the nonlinear schrödinger equation. *Translation from Teoreticheskaya i Matematicheskaya Fizika* **69**, 189.

Betchov, R. 1965 On the curvature and torsion of an isolated vortex filament. *Journal of Fluid Mechanics* **22**, 471–479.

Cieśliński, J. 1992 Two solitons on a thin vortex filament. *Physics Letters A* **171**, 323.

Donnelly, R.J. 1991 **Quantized Vortices in Helium II**. Cambridge University Press.

Dysthe, K.B. & Trulsen, K. 1999 Note on breather type solutions of the nls as models for freak-waves. *Physica Scripta* p. 48.

Fukumoto, Y. & Miyazaki, T. 1986 N-solitons on a curved vortex filament. *Journal of Physical Society of Japan* **55**, 4152–4155.

Gross, E.P. 1961 Structure of a quantized vortex in boson systems. *Nuovo Cimento* **20**, 454–457.

Hasimoto, H. 1972 A soliton on a vortex filament. *Journal Fluid Mechanics* p. 477.

Hirota, R. 1978 Nonlinear partial difference equations. iv. bcklund transformation for the discrete-time toda equation. *Journal of Physical Society of Japan* **45**, 321–332.

Hirota, R. 1982 Bilinearisation of soliton equations. *Journal of Physical Society of Japan* **51**, 323–331.

Hopfinger, E.J. & Browand, F.K. 1982 Vortex solitary waves in a rotating, turbulent flow. *Nature* **295**, 393.

Kelvin, W.T. 1880 Vibrations of a columnar vortex. *Phil. Mag. Ser.* **5** (10), 155–168.

Konno, K. & Ichikawa, Y.H. 1992 Solitons on a vortex filament with axial flow. *Chaos, Solitons & Fractals* **2**, 237–250.

Konno, K., Mituhashi, M. & Ichikawa, Y.H. 1991 Soliton on thin vortex filament. *Chaos, Solitons & Fractals* **1**, 55–65.

Kozik, E.V. & Svistunov, B.V. 2009 Theory of decay of superfluid turbulence in the low-temperature limit. *Journal of Low Temperature Physics* **156**, 215.

Kursa, M., Bajer, K. & Lipniacki, T. 2011 Cascade of vortex loops initiated by a single reconnection of quantum vortices. *Physical Review B* **83**, 014515.

Kuznetsov, E. 1977 Solitons in a parametrically unstable plasma. *Soviet Physics Doklady* **22**, 507.

Leibovich, S. & Ma, H.Y. 1983 Soliton propagation on vortex cores and the hasimoto soliton. *Physics of Fluids* **26**, 3173.

Levi, D., Sym, A. & Wojciechowski, S. 1983 N-solitons on a vortex filament. *Physics Letters A* **94**, 408.

L'vov, V.S. & Nazarenko, S.A. 2010 Spectrum of kelvin-wave turbulence in superfluids. *Pisma v Zhurnal Èksperimental'noi i Teoreticheskoi Fiziki* **91**, 464–470.

Ma, H.Y. 1979 The perturbed plane-wave solutions of the cubic schrdinger equation. *Studies in Applied Mathematics* **60**, 43.

Maksimović, A., Lugomer, S. & Michieli, I. 2003 Multisolitons on a vortex filaments: the origin of axial tangling. *Journal of Fluids and Structures* **17**, 317–330.

Peregrine, D.H. 1983 Water waves, nonlinear schrdinger equations and their solutions. *J. Austral. Math. Soc. Ser. B* **25**, 16.

Pismen, L.M. 1999 **Vortices in Nonlinear Fields: From Liquid Crystals to Superfluids, from Nonequilibrium Patterns to Cosmic Strings**. Oxford University Press.

Pitaevskii, L.P. 1961 Vortex lines in an imperfect bose gas. *Soviet Physics JETP* **13**, 451–454.

Ricca, R.L. 1996 The contibutions of Da Rios and Levi-Civita to asymptotic potential theory and vortex filament dynamics. *Fluid Dynamics Research* **18**, 245–268.

Rios, L. D. 1906 Sul moto d'un liquido indefinite con un filetto vorticoso di forma qualunque. *Rend. Circ. Mat. Palermo* **22**, 117.

Salman, H. 2013 Breathers on quantized superfluid vortices. *Physical Review Letters* **111**, 165301.

Schwarz, K.W. 1988 Three-dimensional vortex dynamics in superfluid $^4$He: Homogeneous superfluid turbulence. *Phys. Rev. B* **38**, 2398.

Umeki, M. 2010 A locally induced homoclinic motion of a vortex filament. *Theoretical and Computational Fluid Dynamics* **24**, 383.

Vinen, W.F. 2000 Classical character of turbulence in a quantum liquid. *Physical Review B* **61**, 1410.